Earthquake Engineering and Structural Dynamics

Experimental Validation of Semi-active Resetable Actuators in a 1/5th Scale Test Structure

Journal:	*Earthquake Engineering and Structural Dynamics*
Manuscript ID:	EQE-08-0116.R2
Wiley - Manuscript type:	Research Article
Date Submitted by the Author:	n/a

Complete List of Authors:	Mulligan, Kerry; University of Canterbury, Mechanical Engineering Chase, J.; University of Canterbury, Mechanical Engineering Mander, John; Texas A&M University, Zachry Dept of Civil Engineering Rodgers, Geoffrey; University of Canterbury, Mechanical Engineering Elliott, Rodney; University of Canterbury, Mechanical Engineering Franco-Anaya, Roberto; University of Canterbury, Civil Engineering Carr, Athol; University of Canterbury, Civil Engineering

Keywords:	hysteresis, semi-active, resetable, base shear, experimental, structural control

Experimental Validation of Semi-active Resetable Actuators in a $\frac{1}{5}^{th}$ Scale Test Structure

Mulligan, K.J Chase, J.G Mander J.B
Rodgers, G.W Elliott, R.B Franco-Anaya R
Carr, A.J

1 Abstract

The seismic performance of a test structure fitted with semi-active resetable devices is experimentally investigated. Shaking table tests are conducted on a $\frac{1}{5}^{th}$ scale four-storey building using 27 earthquake records at different intensity scalings. Different resetable device control laws result in unique hysteretic responses from the devices and thus the structure. This device adaptability enables manipulation or sculpting of the overall hysteresis response of the structure to address specific structural cases and types. The response metrics are presented as maximum 3rd floor acceleration and displacement, and the total base shear. The devices reduce all the response metrics compared to the uncontrolled case and a fail-safe surrogate. Cumulative

probability functions allow comparison between different control laws and additionally allow tradeoffs in design to be rapidly assessed. Ease of changing the control law in real-time during an earthquake record further improves the adaptability of the system to obtain the optimum device response for the input motion and structural type. The findings are an important step to realising full scale structural control with customised semi-active hysteretic behaviour using these novel resetable device designs.

2 Introduction

This paper presents experimental results of shaking table tests conducted on a four-storey $\frac{1}{5}^{th}$ scale model building fitted with semi-active resetable devices. The purpose of this experimental investigation is to validate previous findings from both experimental and analytical studies of these resetable devices at improving structural performance during earthquakes (Hunt (2002), Mulligan et al. (2006), Chase et al. (2006), Rodgers et al. (2007)). A further purpose of these experiments is to better assess the requirements for future implementation of these devices in full-scale prototype structures.

Resetable devices show promise in structural control applications. The unique ability of the resetable devices developed at the University of Canterbury to produce a variety of customised hysteresis loops depending on the device control law has significant advantages for customising control to specific structural applications. In particular, the resulting ability to manipulate or sculpt the overall hysteretic response of the structure is advantageous in addressing specific structural cases and types (Mulligan et al. (2005), Chase et al. (2006), Rodgers et al. (2007)). This ability to manipulate the overall hysteretic behaviour allows the semi-active devices to be effectively applied to a much wider range of structural types than many other semi-active and passive devices or systems. Furthermore, changes to a structure's dynamic behaviour, over time or as a result of damage, can be accounted for by altering the device response, and thus the structures hysteretic behaviour, accordingly. This paper examines the impact of all these capabilities in a 4 Ton (35kN), $1/5^{th}$ scale test structure to experimentally confirm their potential in a realistic larger-scale structure.

3 Resetable Devices

Resetable devices behave essentially as non-linear springs, where the zero or unstressed position can be reset at any point. This resetting releases all the stored energy in the device, resulting in energy dissipation from the structure to which it is attached. More specifically, stored energy that would normally be returned or restored to the structure in the subsequent reversal of motion is released and hence dissipated from the overall structural system (Bobrow and Jabbari (2002)). The advanced devices used in these experiments (Chase et al. (2006)) commonly reset at either the mid point (zero crossing) or maximum (peak) point in each cycle. Changing the configuration of resisting motion and resetting changes the hysteretic response of the device and thus the structure (Rodgers et al. (2007)).

The design of the devices used in these experiments differ from previous resetable devices (Bobrow et al. (1995)) as they have independently acting chambers (Chase et al. (2006)). More specifically, instead of the chambers being connected via a duct and a single valve (Bobrow and Jabbari (2002)), each chamber has a valve and vents directly to atmosphere. Independent control of the device chambers reduces the effect of long energy release times that occur with large motion and high stored energy for larger applications. In addition, the independent chamber design allows for greater variety in the hysteretic response, including different control laws for each chamber (Chase et al. (2006)). Previous research has also examined switching hydraulic oil dampers based on a 1-4 or very similar device control approach and the associated valve operation (Kurino et al. (2004)) , as well as a passive solution using the same device designs and fundamentals that exhibits semi-active characteristics (Kurino et al. (2006)). These latter devices represent full scale applications of resetable systems, although different to the independent chamber controlled 2-4 and adaptive switching approaches considered here.

The specific devices used in this study use air as the working fluid for simplicity, as the surrounding atmosphere serves as a reservoir. This aspect affects the device forces generated but not the overall device behaviour.

The effect of time-lag in valve operation for the resetable devices is an important consideration for the effect on structural response. However, previous research has shown that time-lag induced by the valve reset command and valve actuation are on the order of 20 ms (Rodgers et al. (2007), Barroso et al. (2003b)), which will therefore not measurably impact the response of the experimental structure that is first-mode dominant, with fundamental period of 0.44 seconds (Franco-Anaya et al. (2007)).

3.1 Resetable Device Control Law Definition

The control laws available with this independent chamber configuration results in different types or shapes of hysteretic response. Dividing a sinusoidal motion cycle into four quadrants and selectively resisting motion in different quadrants creates these different hysteretic responses. More specifically, if all motion is resisted, with resetting at the peak displacement, the resulting hysteretic response is the parallelogram as shown in Figure 1. This control law and hysteretic loop results from the originally proposed single valve configuration of Bobrow and Jabbari (2002) and analytically examined in structural applications by Hunt (2002) and Barroso et al. (2003b). It should be noted that Figure 1 presents an ideal device model with linear stiffness, whereas a real device will exhibit non-linear stiffness (Chase et al. (2006), Rodgers et al. (2007), Mulligan (2007)). With all motion resisted the device provides restoring forces in all four quadrants of the force-displacement plot and is hence termed the 1-4 (one through four) control law. Note that this simplest of device control laws does not require independent chamber control.

Alternatively, resisting motion only on the return motion of the device (motion towards the rest or zero position of the structure from a peak) results in the hysteretic response shown in Figure 2. This control law results in the device providing restoring forces in only the 2nd and 4th quadrants and is thus termed the 2-4 (two, four) control law. This control law has the additional benefit over the 1-4 law, as not only is energy dissipated by the device but, the maximum restoring force occurs when the structural force is not a maximum. Hence, the total force required to be resisted by the

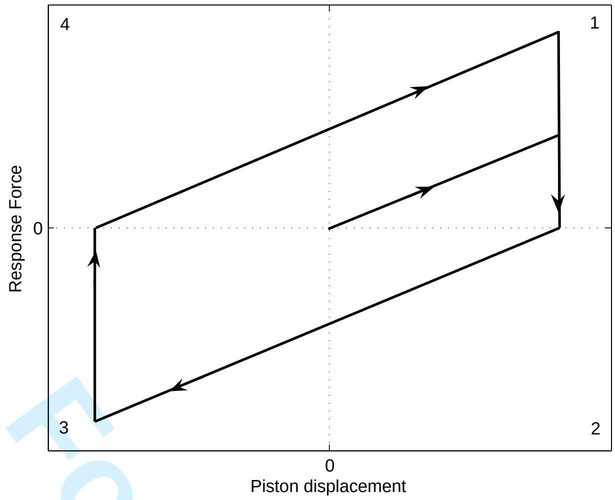

Figure 1: Ideal hysteretic response of resetable device resisting all motion. The active chamber valve is opened, releasing the stored energy, at the peak piston displacement for each cycle. Quadrant numbers are shown numbering in a clockwise direction.

foundations or base shear is not increased with the addition of resetable devices using this form of control (Rodgers et al. (2007), Mulligan (2007)). In contrast, the 1-4 law may significantly increase the overall storey and base shear demand in the lower storeys and foundations, respectively .

In summary, Figure 3 illustrates these two control laws and overall hysteresis loops. This schematic shows the force displacement response of a linear structure with the addition of a resetable device and the resulting maximum base shear. Figure 4 shows the schematic design for these independent chamber controlled resetable devices (Chase et al. (2006) and Mulligan (2007)).

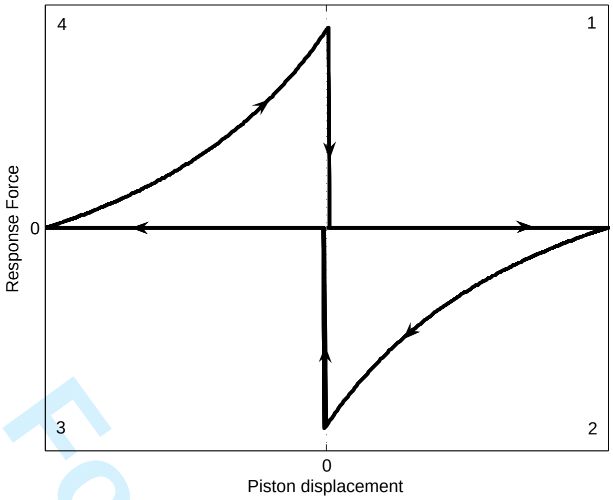

Figure 2: Ideal hysteretic response of resetable device resisting only return motion. The active chamber valve is closed at the peak displacement and opened, releasing the stored energy, at the zero piston displacement for each cycle. Quadrant numbers are shown numbering in a clockwise direction.

4 Experimental Investigation

4.1 Experimental Layout and Device Architecture

The experimental $\frac{1}{5}^{th}$ scale model four-storey moment resisting steel frame building structure, shown schematically in Figure 5, is comprised of two bays, one short and one long. The structure was designed to have a similar natural period to a full-scale structure. To achieve this objective, additional mass is added to the floor diaphragms, resulting in a natural period of 0.44 seconds and a corresponding equivalent viscous damping ratio of 1.21% (Franco-Anaya et al. (2007)). Second and third modes occur at approximately 0.11 and 0.05 second periods respectively. It should be noted that the equivalent viscous damping values have been observed to be weakly input magnitude dependent, so the assumption of viscous damping may not be an appropriate

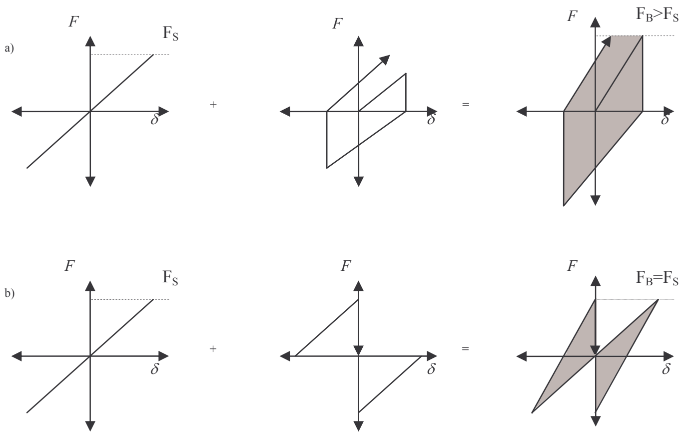

Figure 3: Change in hysteretic response of a linear single-degree-of-freedom structure with the addition of a resetable device (Chase et al. (2006)). The shaded area indicates the amount of energy dissipated per structural motion cycle. F_S is the maximum structural force, F_B is the maximum total base shear of the structure and damping device combination. The first row shows the result of the 1-4 control method. Note the increase in the overall resulting force (F_B) compared to the structure alone maximum force (F_S). The second row shows the result with the 2-4 control law enabled by the independent chamber design. In this case F_B is not increased compared to F_S, a significant advantage where an increase in foundation demand is undesirable or potentially damaging.

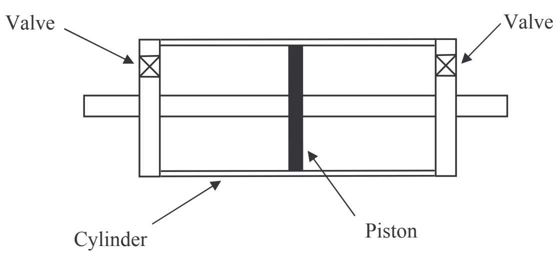

Figure 4: Schematic of independent chamber design, one valve per chamber.

model. To further model the realistic, non-linear behaviour of a full-scale structure the test structure is designed with yielding fuses at each connection and at the mid-point of each long span to replicate the plastic hinge behaviour (Kao (1998), Rodriguez et al. (2006)).

The resetable devices were connected via a near rigid buckling-restrained brace between the ground and the third floor, spanning the entire length of the long side of the structure. This configuration was chosen following an extensive non-linear finite element examination of several device architectures (Franco-Anaya et al. (2007)). The semi-actively controlled brace basically connects the seismic centre of mass of this first mode dominant structure to the ground. One brace with a device was installed on each long side of the structure to remove the potential for any torsional motion.

Each device was controlled independently, creating a simple decentralised structural control method. Each device was controlled depending on the relative displacement between the ground and the third floor attachment point, as measured locally across the device. Thus, torsional effects can be at least partly negated as either device provides a larger restoring forces if a greater displacement occurs on one side of the structure.

Structural response accelerations to ground motion were measured at each floor using accelerometers recording data at a 2kHz sampling rate. Absolute displacements were monitored by linear potentiometers attached to a 'strong frame' (see Figure 5). The linear potentiometers measured displacements at the midpoint between each floor and the roof and are also referenced to a potentiometer measuring the shake table displacement. All data was sampled at 1kHz using a dSpace™system.

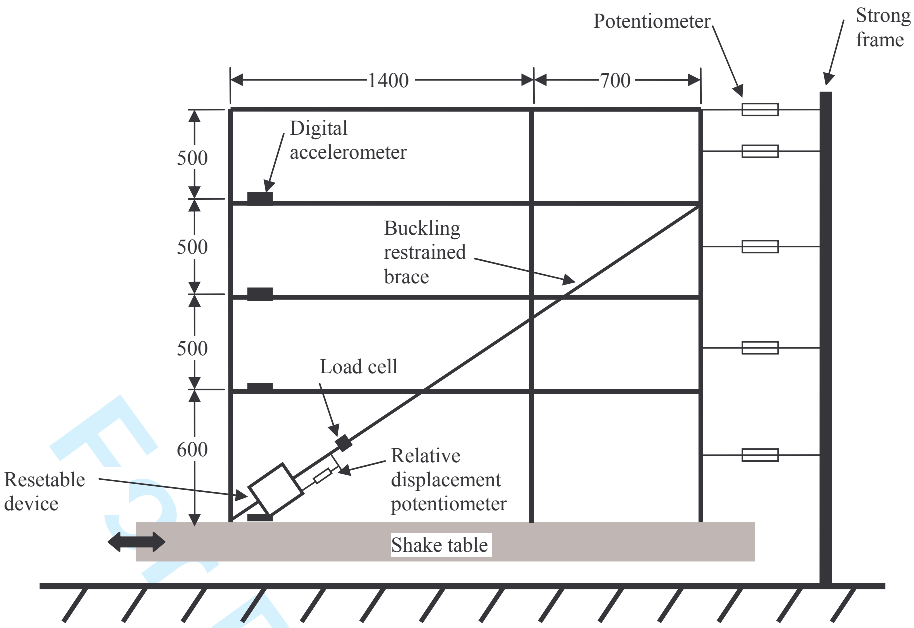

Figure 5: Schematic of the test structure indicating the instrumentation configuration. All dimensions are in millimeters.

Displacements at each floor level were inferred by linear interpolation of adjacent storey (midpoint) values. These interpolated values were verified to be accurately represent the floor level displacements by comparison with the double integration of the accelerometer data, as well as from the results of other studies (Kao (1998), Rodriguez et al. (2006)). Figures 5 and 6 show a schematic and photograph of the structure indicating the placement of the measuring instruments and the resetable devices. In addition, Figure 7 shows a close up of one resetable device, as installed on the test structure.

4.2 Control Laws

The experimental investigative nature of this research led to a variety of control laws being implemented. The control laws implemented were the

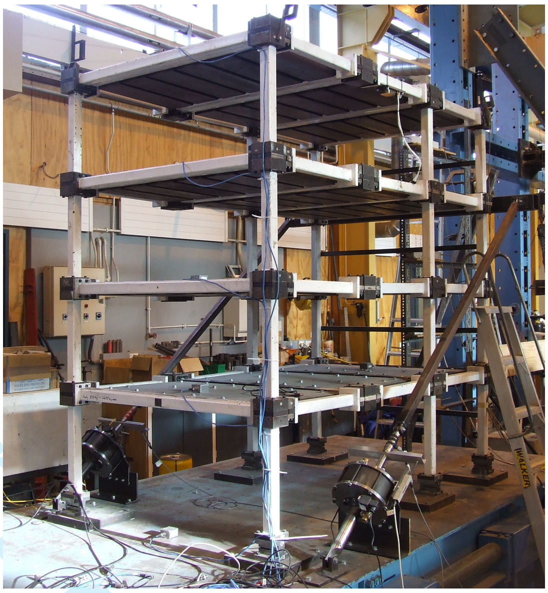

Figure 6: Photograph of the test structure on the shake table with a resetable device attached to each side of the structure between the ground and (3^{rd}) floor via rigid tendons.

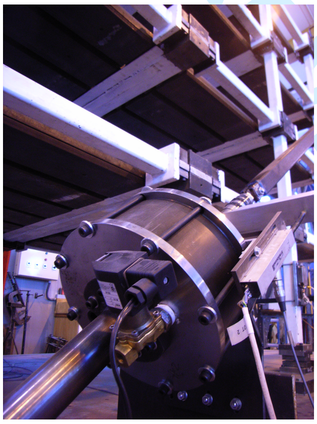

Figure 7: Closeup of a resetable device installed on the test structure. The linear transducer on the left side measures displacement across the device from which relative (3^{rd}) floor motion (to ground) can be inferred.

1-4 and 2-4, and a configuration where the control law was switched from the 1-4 case to the 2-4 case based on structural response motion across the device. Results were also obtained for a fail-safe mode with all valves closed, representing the scenario if power is lost to the devices, which turns the devices into pneumatic springs with minimal dissipation.

Finally, the uncontrolled response was obtained. The uncontrolled response would ideally occur with the entire device and tendon arrangement removed. However, finite element analysis predictions of large structure motion indicated that significant deformation of the yielding fuses would occur for some earthquake input motions used. For these larger magnitude ground motions the devices were used with all valves open as a surrogate for the fully uncontrolled case. This valves open configuration creates very small device forces from friction and air damping through open orifices.

4.3 Earthquake Ground Motions

The experiments were conducted on the University of Canterbury 5-tonne (20-tonne pay-load capacity) single-axis shake table. Using appropriate record modification techniques, accurate control of the table, accounting for table-structure interaction was achieved using the recently developed control strategies outlined in Chase et al. (2004). The behavior attributes and dynamics of the test structure are well known and have been thoroughly documented by Rodriguez et al. (2006). What is interesting about the experimental physical model is that while on the one hand the structure has a reduced physical size (dimensionally it is 20% full size), on the other hands its dynamic characteristics have been chosen to give 1:1 (model:prototype) similitude. This constant-time similitude performance attribute is beneficial when investigating real-time implementation issues concerned with electro-mechanical switching and other inevitable phase-lag delays associated with semi-active control of structures.

A total of 27 earthquake records derived from different intensity scalings of four measured earthquake ground motions were utilised in the experiments. These records are detailed in Table 1, which indicates the measured motion, the scaled percentage of the original record, the peak ground acceleration (PGA) measured during the experiment, and the spectral displacement of a single degree-of-freedom, 0.4 second period structure. Note, a 0.4 second period, as opposed to the 0.6 second period of the uncontrolled test structure, is used to determine the SA and SD values due to an assumed increase in structural stiffness resulting from the attached tendon. The measured table motions are used as an indication of the intensity, rather than the original record, as measured experimental values better indicate the motion experienced by the structure, where any differences may occur between the input and actual table motion (Chase et al. (2004)).

Note that the PGA of the 5% Slymar record is greater than that for the 10 and 15% records. This anomaly is due to a short, sharp spike that occurred during the experimental procedure that was not present in the input command to the shake table. This spike is most likely due to spurious shake table motion resulting from a command saturating the table valve or electronic control failure. An approximated value derived from original acceleration data is shown in brackets in Table 1 and is the value used in further analysis with this record.

Minor modification of some earthquake records was required to ensure the shake table was capable of producing the required motion. The limiting factor for reproducing motion is the velocity achievable by the shake table, due to servo-valve saturation that occurs at 0.24m/s (Chase et al. (2004)). Therefore, portions of any earthquake records that exceed this value are modified such that the velocity does not exceed this saturation level. This process modifies only veryshort portions and maximises retention of the original acceleration profile.

4.4 Response Metrics

The structural performance metrics of interest include the maximum 3rd floor displacement and acceleration, and the total base shear. These metrics indicate the damage to the structure, the occupants and non-structural elements, and the foundations of the structure, respectively. Typically, a reduction in one of these metrics can result in a concomitant increase in another metric (Rodgers et al. (2007)). For example, the addition of resetable devices can significantly decrease the displacement response of a structure at the expense of increasing the acceleration (Hunt (2002), Barroso et al. (2003b)). However, utlising the customised control methods possible with the specific resetable device designs used in this research, it is possible to achieve decreases in all metrics, or large reductions coupled with only small increases.

Normalising these performance metrics results to the intensity measure of

Table 1: Ground motion records used for shake table analysis of a $\frac{1}{5}^{th}$ scale structure with a resetable device damping system. El Centro, Kobe, Taft and Sylmar records were used with different percentages of each record. The magnitude of each record is determined by the percentage of the original record, the peak ground acceleration (PGA) recorded during the test, and the spectral displacement (SD) intensity measure for a single-degree-of-freedom structure with a natural frequency of 2.5Hz and 5% damping.

	% of record	PGA (recorded)	SA (2.5Hz)	SD (2.5Hz)
El Centro 1940 NS	10	0.8451	0.06	0.0024
	20	0.11	0.1	0.0048
	30	0.13	0.18	0.0073
	40	0.15	0.24	0.0097
	50	0.17	0.30	0.0121
	60	0.22	0.36	0.0145
	70	0.27	0.43	0.0170
	80	0.30	0.49	0.0194
	90	0.31	0.59	0.0218
	100	0.36	0.60	0.0242
Kobe 1995 N00E	5	0.09	0.11	0.0045
	10	0.12	0.23	0.0090
	15	0.15	0.34	0.0135
	20	0.19	0.45	0.0180
	25	0.22	0.57	0.0225
	30	0.26	0.68	0.0269
	35	0.29	0.79	0.0314
Taft 1952 S21W	20	0.15	0.070	0.0028
	40	0.28	0.14	0.0056
	60	0.38	0.21	0.0083
	80	0.51	0.28	0.0111
Sylmar 1994 0° Ch 9	5	0.14 (0.04)	0.10	0.0040
	10	0.10	0.20	0.0081
	15	0.12	0.30	0.0121
	20	0.15	0.41	0.0162
	25	0.19	0.51	0.0202
	30	0.23	0.61	0.0242

the ground motion record enables easy, rapid comparison across all ground motions. This normalisation also allows comparison with spectral analysis examinations of these resetable devices (Rodgers et al. (2007)). The results can then be presented as cumulative distribution functions, which are then able to be more readily incorporated into standard hazard analysis and performance based design (Barroso et al. (2003a), Rodgers et al. (2007)).

5 Results and Discussion

Before extensive testing or detailed processing of results could take place it was necessary to validate that the resetable devices were operating as expected. The force-displacement of the devices was plotted and checked against the results of previous experimental characterisation tests.Figure 8 shows the previously characterised experimental and non-linear modelled device response for the 2-4 control law (Mulligan (2007)) compared with a selected portion of a device response from the shake table testing. Note that the device operation, which uses the same software controller and sensors in both experiments, has the same overall behaviour. The main differences occur due to the variable speed across the device and non-sinusoidal input for the earthquake ground motion, compared to the characterisation test. Hence, the devices are seen to behave, under control, as expected in these experiments.

The displacement and base shear response metrics for each scaled ground motion and control law are plotted versus the intensity measure of the record in Figure 9, along with the linear (displacement) or non-linear (base shear)

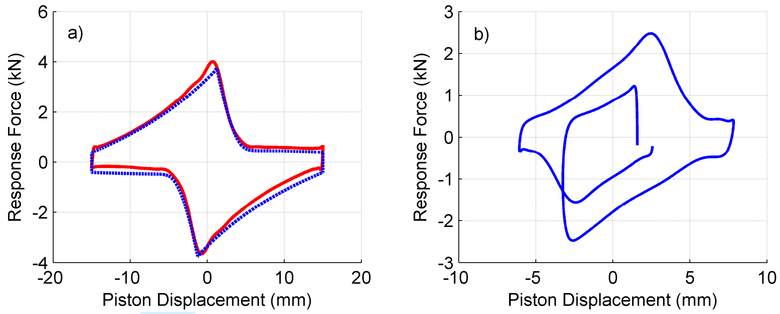

Figure 8: Comparison of a) previous experimental and modelled device response (Mulligan (2007)) and b) a portion of the in-service device response to 2-4 control during shake table testing

least squares fit. Uncontrolled only show 4 results due to the expected fuse yielding during large structural motion as described previously.

The structure base-shear and displacement response with all the control laws and the uncontrolled case are summarised readily compared in Figures 10 and 11, which bring together the least squares fit lines of Figure 9. As expected the *uncontrolled* response produced the greatest maximum 3rd floor displacement response for each applied intensity measure in Figure 11, whereas the 1-4 control law has the lowest response in this metric. Furthermore, the *fail-safe* mode and the *1-4* control law produced very similar maximum 3rd floor displacement response. This indicates the stiffness of the resetable devices is comparable using both of these two-valve control configurations. This result might be expected as the 1-4 law acts over the entire response cycle. Thus, the only difference between 1-4 control and fail-safe case is the resetting energy dissipation.

As expected, the 2-4 control law results in a larger displacement response

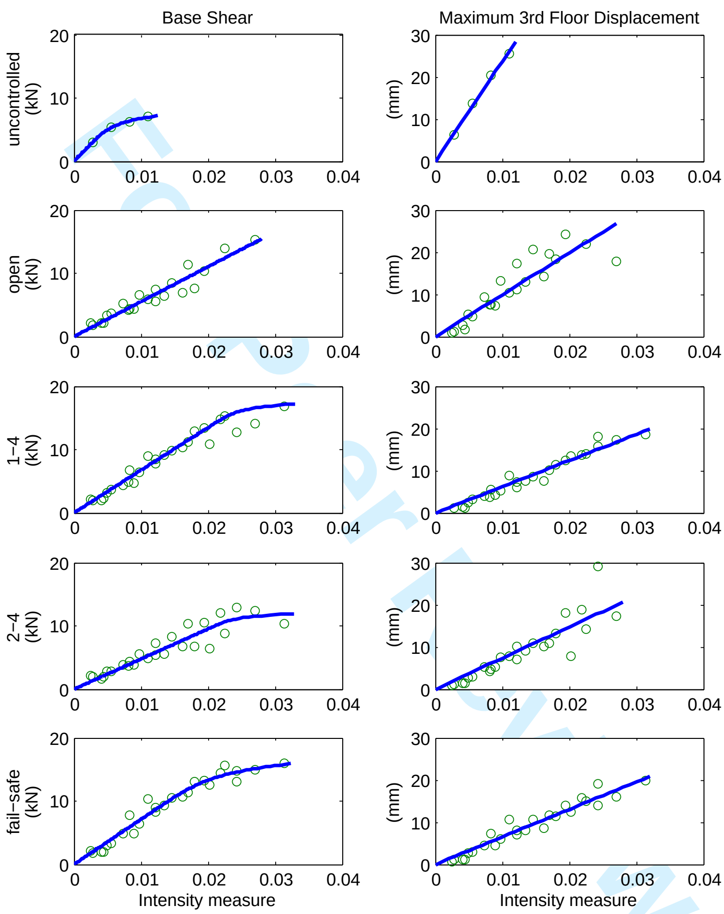

Figure 9: Base shear and maximum 3rd floor displacement for all control types and the uncontrolled case including the least squares fit relative to the spectral displacement intensity measure.

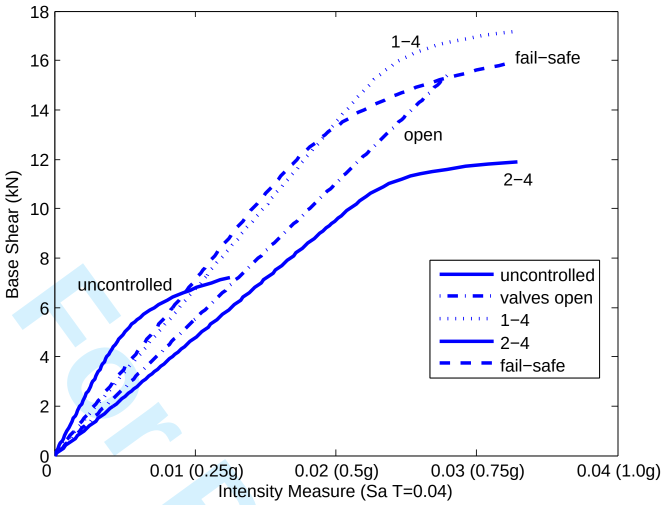

Figure 10: Least squares fit of base shear comparing all control types and the uncontrolled case relative to the spectral displacement intensity measure.

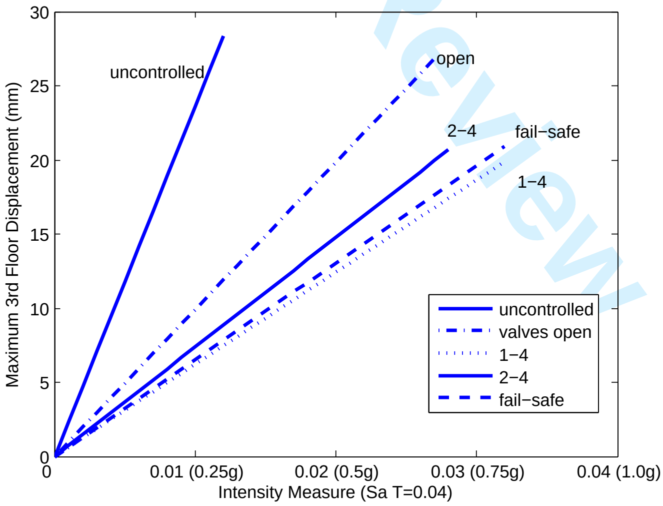

Figure 11: Least squares fit of maximum 3rd floor displacement comparing all control types and the uncontrolled case relative to the spectral displacement intensity measure.

to the 1-4 (best case). This difference occurs because the 2-4 control law only stores and releases half of the potential amount of force on valve release (reset) as it resists only half the motion of a 1-4 device (Rodgers et al. (2007)). Despite this apparent 50% efficiency of the 2-4 control law with respect to the fully resisting 1-4 control case, the experimental results show that there is only a 10% improvement in displacement response reduction when comparing the 2-4 to 1-4 control laws. However, as shown in Figure 10, when comparing base shear forces the 1-4 cotnrol law leads to shear demands that are 33% higher than the 2-4 control law. Clearly the 2-4 control law has the best reduction in base shear demand.

Interestingly, the 2-4 law also results in a decrease in base-shear demand per unit intensity measure compared to the valves open response that is used as a surrogate uncontrolled response for many ground motions. This result is due to the overall reduction in motion achieved with the 2-4 control law compared to the valves-open response. In contrast, the 1-4 case base is larger than this valves open, surrogate uncontrolled case. Hence, explicitly and specifically resisting less motion results in an overall lower base shear demand.

Overall, although trends are discernable, it is difficult to make design decisions from data represented in the manner provided in Figures 9, 10 and 11. Cumulative distribution functions (CDF) give the probability of exceedence of a given metric for a given ground motion intensity and hence also provide a measure of the dispersion of the observed results. Figure 12 shows the observed data plotted in the form of cumulative distributions for the base-shear, maximum 3rd floor displacement and peak 3rd floor acceleration for

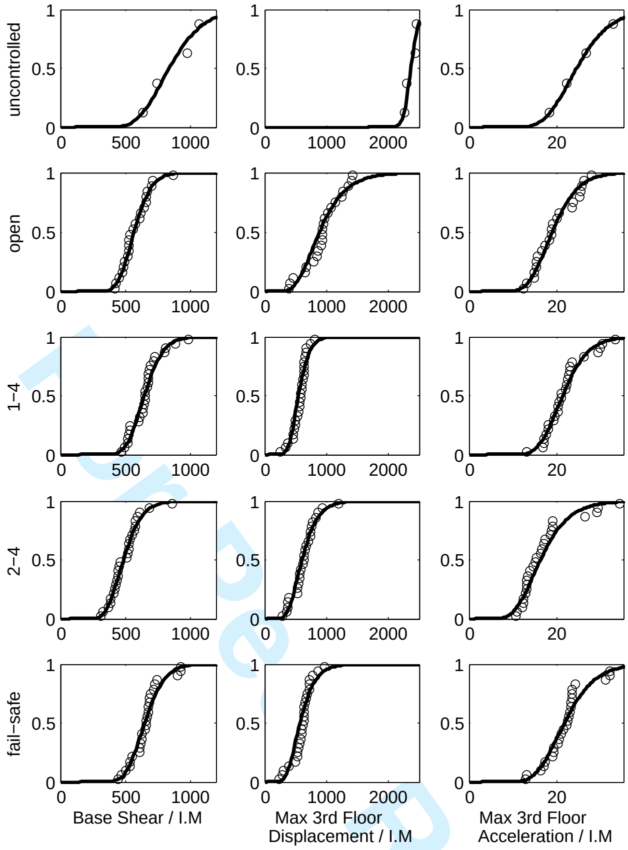

Figure 12: Cumulative distributions of base shear (left column), maximum 3^{rd} floor displacement (center column) and 3^{rd} floor acceleration (right column). The experimental results (in circles) are normalised and plotted with respect to their intensity measure. Fitted to each set of results is a lognormal distribution (solid line).

the uncontrolled case and all control methods. Fitted to these experimentally observed results are lognormal cumulative distributions. The lognormal distribution is a two parameter model described by a median ($\hat{x}$) and a lognormal standard deviation ($\sigma_{\ln x} = \beta$) sometimes referred to as the dispersion factor.

To compare the merits of each control method, Figures 13 to 15 show fitted CDF for the base-shear, maximum 3rd floor displacement and peak 3rd

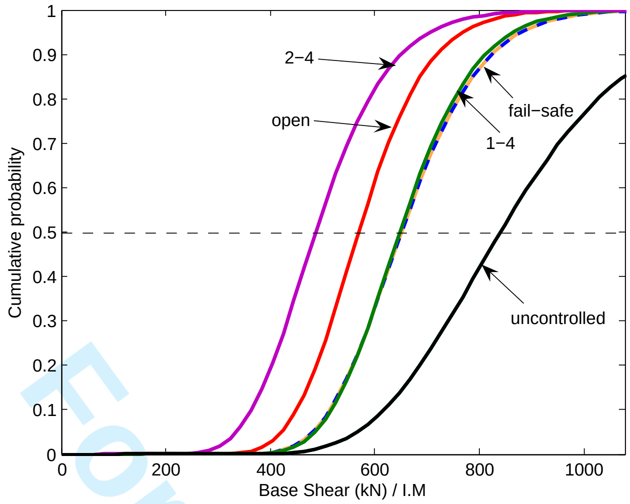

Figure 13: Lognormal base shear cumulative probability functions.

floor acceleration, respectively. In addition, Table 2 shows for each control law the median ($\hat{x}$), dispersion factor (β), mean ($\bar{x} = \hat{x}\exp(1/2\beta^2)$) and the mean expected response normalised to the 'valves-open' and uncontrolled case. In Figures 13 to 15, the CDF y-axis values indicates probability of exceeding a given metric for a given ground motion intensity. Thus, the structural demands are reduced as the probability function moves towards the left upper corner of the plot.

Figure 14 indicates that the addition of the buckling restrained brace and device to the structure, whether the device is controlled or is simply supplying some small restoring force, as in the valves open case, the maximum 3rd floor displacement is reduced. This result is expected as the buckling restrained brace and device slightly increases the stiffness of the structure, thus reducing the displacement for the same intensity measure intensity measure.

The 1-4 control shows the best response in reducing the maximum 3rd floor displacement with a lognormal mean of 549mm/I.M compared to a

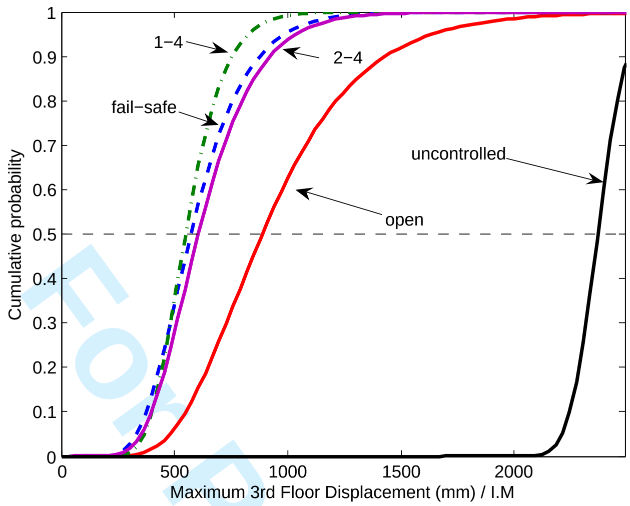

Figure 14: Lognormal maximum third floor displacement cumulative probability functions.

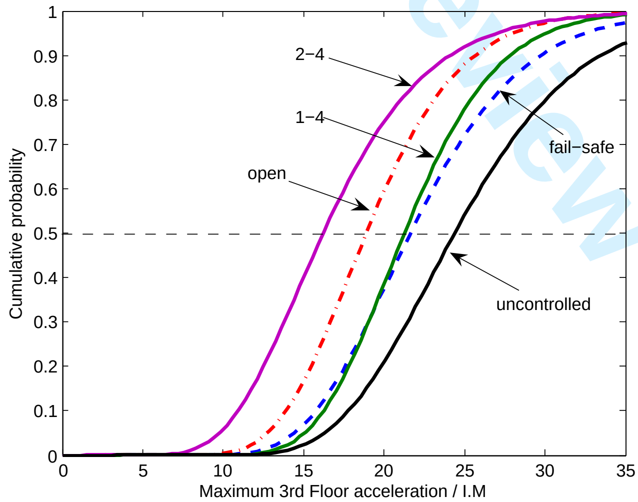

Figure 15: Summary of experimental results for each control case.

Table 2: Lognormal mean ($\hat{x}$) and multiplicative variance (σ) for base shear, maximum 3rd floor displacement and acceleration for each control case.

Control Law		Uncontrolled	Open	1-4	2-4	Fail-safe
Base Shear Force (kN)	$\hat{x}$	839	568	647	486	650
	β_{RD}	0.239	0.182	0.174	0.223	0.182
	$\bar{x}$	863	578	657	498	661
	Ratio 1	1.49	1.00	1.14	0.86	1.14
	Ratio 2	1.00	0.67	0.76	0.58	0.77
3^{rd} Floor Displacement (mm)	$\hat{x}$	2368	887	549	605	573
	β_{RD}	0.039	0.372	0.247	0.329	0.329
	$\bar{x}$	2370	950	566	639	605
	Ratio 1	2.49	1.00	0.60	0.67	0.64
	Ratio 2	1.00	0.40	0.24	0.27	0.36
3^{rd} Floor Acceleration (mm/s)	$\hat{x}$	24	19	21	16	22
	β_{RD}	0.247	0.239	0.207	0.307	0.247
	$\bar{x}$	25	20	21	17	23
	Ratio 1	1.27	1.00	1.10	0.86	1.16
	Ratio 2	1.00	0.79	0.87	0.68	0.92

$\hat{x}$ = median value
$\bar{x} = \hat{x}\exp(0.5\beta_{RD}^2)$ = mean (expected value)
Ratio 1 = ratio of mean value with respect to the Open case
Ratio 2 = ratio of mean value with respect to the Uncontrolled case

values of 887mm/I.M and 2368mm/I.M for the valves open and uncontrolled responses respectively. In addition, the 1-4 control law results in the lowest dispersion for this metric, excepting the uncontrolled response. This anomaly of a low dispersion for the uncontrolled response is due to the small number of data points (four) available to derive this data. Moreover, only relatively low intensity records were able to be used for the uncontrolled structure to ensure that significant damage through inelastic response did not occur, further reducing the dispersion.

The fail-safe and 2-4 control modes have similar results to the 1-4 case, although with slightly larger dispersions. The mean values are comparable to the 1-4 case, particularly when compared to the valves open or uncontrolled response.

Table 3 presents an overall summary of the experimental results which are tabulated for each structural control law and the uncontrolled condition. Listed are response metrics for base shear force, maximum 3^{rd} floor displacement (building drift) and acceleration. In Table 3 the median (50^{th} percentile values in Figures 12 to 14)$\hat{x}$, the mean calculated assuming a lognormal distribution such that $\bar{x} = \hat{x}\exp(0.5\beta_{RD}^2)$ where $\beta_{RD}^2 =$ experimentally observed lognormal standard deviation (also known as the dispersion factor) of randomness of the demand. Also listed in Table 3 are normalized ratios representing response relative to the *Valves open* (*Ratio* 1) and *Uncontrolled* (*Ratio* 2) cases.

From a general examination of the *Ratio* 2 values listed in Table 3 it is evident that some form of control is beneficial in reducing all response metrics. There is generally an approximately 30%, 70% and 20% reduction in base shear, displacement and floor acceleration, respectively. Particularly notable is the significant reduction in displacement response. For structures in high seismic zones these reductions translate into a damage reduction for both the structure, and internal fittings such as glazing and fixed partitions.

However, it is the examination of *Ratio* 1 in Table 3 that gives insight into the effectiveness of each of the control laws. Although the 1-4 control law is the most effective in reducing displacement response and hence in mitigating structural damage, it is only marginally better than the 2-4 and fail-safe conditions. The 2-4 control law is the only case where reductions in all three performance response metrics are observed. Not only are the response displacements reduced, but also the base shear and floor accelerations are reduced. The acceleration and base shear reductions imply smaller foundations might be constructed and less acceleration-sensitive damage to contents will result, respectively. For retrofit cases, base shear reductions have the important potential benefit of reducing the likelihood of exceeding an older foundations design limits.

A spectral analysis by Rodgers et al. (2007) of these resetable devices indicated the potential of these different control laws at reducing a wide range of response metrics of interest. Collation of the experimental validation results of this study in a comparison with these spectral analysis results shows a good correlation between analytical and experimental values, as shown in Figure 16. This correlation provides added confidence in using these spectral analysis results in further design and applications of different resetable device types.

One remaining question is: How well will the 2-4 control mitigate response of near-field earthquakes with large acceleration pulses early in the record, compared with 1-4 control. This question remains because one would intuitively expect the system to operate more effectively under 1-4 control by actively reducing large, damaging initial movements away from its initial static position that can be induced in such events. This approach would however place increased base shear demand on the structure. One possible answer is to have a mixed control law, combining the best attributes of 1-4 and 2-4 control.

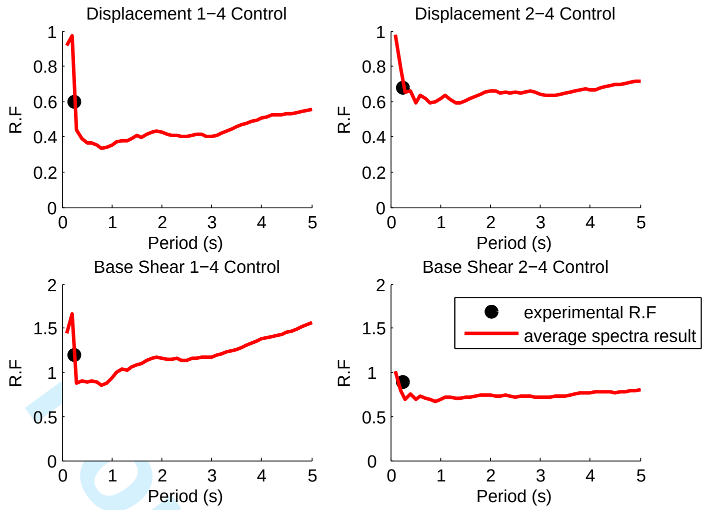

Figure 16: Experimental reduction factors for displacement and base shear on the spectra developed by Rodgers et al. (2007) for maximum third floor displacement and base shear for the 1-4 and 2-4 control laws. These comparisons shows good correlations and validate the prior analytical work.

5.1 Switching Control Laws

Overall, the results so far show a trade off between reducing displacements, and reducing acceleration and base-shear demands, similar to the results of other studies (Hunt (2002), Barroso et al. (2003a), Rodgers et al. (2007)). The 2-4 control law significantly reduces or eliminates this tradeoff. However, given the ease of changing between different control modes in real-time during an event using only software, it was proposed to optimise the device response depending on the structural motion. More specifically, high intensity ground motions, typically resulting in large initial impulse displacements, are best resisted using the 1-4 control law, while the remainder of a given near-field ground motion might be best resisted with the 2-4 control method.

The optimisation of the control law and switching configuration is dependent on the structure type and ground motion. Therefore, it is important to understand the capacity of the structure and the demands resulting from the ground motion. For this prototype structure, the optimum response is to reduce the displacements as much as possible without increasing the base-shear demand.

Hence, this adaptive device control proposal was tested using the El Centro 80% ground motion record, which possesses a large pulse soon after the motion commences. This ground motion was used because it has two relatively long strong motion periods. In addition, its RMS acceleration is thus quite high. In combination with a relatively large initial motion it was an acceptable ground motion record for this one unique test.

The control law was initially started in a 1-4 mode. It was then switched from the 1-4 to the 2-4 when the displacement across the device exceeded 7mm in both directions. This displacement corresponds to a relatively large structural motion for this test structure. Thus, any initial large structural motion is resisted with the 1-4 control law, reducing the maximum displacements, while the remainder of the ground motion record is resisted with the 2-4 control law, reducing or minimising the base shear. Table 3 indicates that by using this adaptive switching configuration the maximum 3rd floor displacement *and* the base shear is reduced compared to the 1-4 case. In addition, although the base shear with the switching case is not as low as with the 2-4 control law alone, the displacement is greatly reduced from that case.

Finally, Table 3 also gives the cumulative base shear. This metric is a measure of the total loading on the foundations for the duration of the earthquake. The switching device control law case has a cumulative base shear value that is between the 1-4 and 2-4 cases, as might be expected. This result further illustrates the tradeoffs between the reductions possible with each control law configuration. It is suggested that although the mixed control law shows promise, it should bear investigation on a structure specific case-by-case basis. In this way, a more optimum implementation may be achieved by taking best advantage of the devices capability in any given structural response condition.

Table 3: Maximum base shear, cumulative base shear, and maximum 3rd floor displacement for the 1-4, 2-4 and switching control laws for the 80% El Centro (1940 NS) ground motion record. (Note, the switching control law changes from the 1-4 to the 2-4 case when the relative displacement across the device exceeds 7mm in both directions.)

Control type	Maximum Base Shear (kN)	Cumulative Base Shear (kN)	Maximum 3rd Floor Displacement (mm)
1-4	13.5	76	12.4
2-4	9.6	63	18.0
switching 1-4 to 2-4	11.0	71	12.1

6 Conclusions

Large-scale testing of resetable devices has illustrated the potential of semi-active resetable devices as structural control elements. The addition of two devices in a buckling restrained brace arrangement greatly improves the structural performance of a $\frac{1}{5}^{th}$ scale moment resisting steel frame model building under a variety of earthquake loads and intensities. The variety of device control laws offers flexibility in the controlled structure response obtained by sculpting or reshaping the overall hysteretic behaviour. Each control law specifically targets reductions in a particular metric, typically with the tradeoff of a increase in another metric. However, the most significant results arise from the 2-4 control law. This control case presents favourable results that show improvements in *all* performance metrics, base shear, displacement, and acceleration, as expected from prior spectral analysis and finite element analysis, although with lesser gains in some metrics. This result is particularly important for retrofit applications, where reductions in the structural displacement are necessary to reduce structural damage, but the foundations may have insufficient strength to meet the resulting increased demand.

The tradeoff between improvements in some metrics, with corresponding degradation or reduced gains in other metrics, is addressed by switching control methods depending on the structural motion resulting from the ground motion input. In particular, this switching method gives comparable results to the best improvements in all performance metrics obtained with the standard device control methods. Hence, this switching control method further confirms the adaptive capabilities of the semi-active resetable devices developed to adapt to changing structural demands due to non-linear behaviour from large ground motion pulses or structural degradation over time.

The fail-safe case presents the worst case scenario with a control system utilising resetable devices. This case occurs when the power to the devices fails or the control system malfunctions. The structural dynamics with the fail-safe mode are still favourable over the uncontrolled or surrogate uncontrolled (valves open) cases for this structure, indicating the robustness in using such resetable device control systems. Note that these devices require very little power and could be run from readily available batteries.

Overall, these shake table experiments have shown the efficacy of these novel semi-active resetable devices as a structural control method. The experiments are the first application of this novel type of semi-active resetable device tested in a realistic physical model under realistic shaking conditions. They are also the first experiments to utilise and validate the customised hysteresis loops enabled by this novel device design. Thus, the findings are an important step to realising full scale structural control with customised semi-active hysteretic behaviour using these novel semi-active resetable devices, or any other device capable of providing these unique capabilities.

References

Barroso, L. R., Chase, J. G., and Hunt, S. (2003a). Probabilistic seismic hazard analysis of semi-active controlled 9-story steel moment-resisting structure. In *16th ASCE Engineering Mechanics Conference*, University of Washington, Seattle.

Barroso, L. R., Chase, J. G., and Hunt, S. (2003b). Resettable smart dampers for multi-level seismic hazard mitigation of steel moment frames. *Journal of Structural Control*, 10:41–58.

Bobrow, J. E. and Jabbari, F. (2002). Vibration suppression with resettable device. *Journal of Engineering Mechanics*, 128(9):916–924.

Bobrow, J. E., Jabbari, F., and Thai, K. (1995). An active truss element and control law for vibration suppression. *Smart Materials and Structures*, 4(4):264–269.

Chase, J. G., Hudson, N. H., Lin, J., Elliot, R., and Sim, A. (2004). Nonlinear shake table identification and control for near-field earthquake testing. *Journal of Earthquake Engineering,*, Vol. 9(No. 3):1–22.

Chase, J. G., Mulligan, K., Gue, A., Alnot, T., Rodgers, G., Mander, J. B., Elliot, R., Deam, B., Cleeve, L., and D, H. (2006). Re-shaping hysteretic behaviour using semi-active resettable device dampers. *Engineering Structures*, 28(10):1418–1429.

Franco-Anaya, R., Carr, A., Mander, J. B., Chase, J. G., Mulligan, K., and Rodgers, G. (2007). Seismic testing of a model structure with semi-active resetable devices. In *New Zealand Society for Earthquake Engineering*, Palmerston North, New Zealand.

Hunt, S. (2002). *Semi-Active Smart-Dampers and Resetable Actuators for Multi-Level Seismic Hazard Mitigation of Steel Moment Resisting Frames.* Master of Mechanical Engineering, University of Canterbury.

Kao, G. C. (1998). *Design and shaking table tests of a four-storey miniature structure built with replaceable plastic hinges.* Master of Civil Engineering, University of Canterbury.

Kurino, H., Matsunaga, Y., Yamada, T., and Tagami, J. (2004). High performance passive hydraulic damper with semi-active characteristics. In *Proceedings, 13th World Conference on Earthquake Engineering*, Vancouver, British Columbia, Canada.

Kurino, H., Yamada, T., Matsunaga, Y., and Tagami, J. (2006). Switching oil damper with automatic valve operation system for structural control. In *4th World Conference on Structural Control and Monitoring*, University of California, San Diego.

Mulligan, K. (2007). *Experimental and Analytical Studies of Semi-Active and Passive Structural Control of Buildings*. PhD, University of Canterbury.

Mulligan, K., Chase, J. G., Gue, A., Alnot, T., Rodgers, G., Mander, J. B., and Elliot, R. (2005). Large scale resetable devices for multi-level seismic hazard mitigation of structures. In *9th International Conference on Structural Safety and Reliability*, Rome, Italy.

Mulligan, K., Fougere, M., Mander, J. B., Chase, J. G., Deam, B., Danton, G., and Elliot, R. (2006). Hybrid experimental analysis of semi-active rocking wall systems. In Brabhaharan, P. and Deam, B., editors, *Remembering Napier 1931, Building on 75 Years of Earthquake Engineering in New Zealand*, Napier, New Zealand. New Zealand Society for Earthquake Engineering.

Rodgers, G., Mander, J. B., Chase, J. G., Mulligan, K., Deam, B., and Carr, A. (2007). Re-shaping hysteretic behaviour - spectral analysis and design equations for semi-active structures. *Earthquake Engineering and Structural Dynamics*, 36(1):77–100.

Rodriguez, M., Restrepo, J., and Blandon, J. (2006). Shaking table tests of a four-story miniature steel building - model validation. *Earthquake Spectra*, 22(3):755–780.